Hindawi
Andrologia
Volume 2024, Article ID 6084885, 11 pages
https://doi.org/10.1155/2024/6084885

Research Article

Hyperuricemia Induces Reproductive Damage in Male Rats through Zinc Homeostasis Imbalance and Oxidative Stress

Liger Te,[1] **Yuejia Li**,[1] **Junsheng Liu**,[1] **Xuan Liu**,[1] **Ming Zhao**,[2] **Shusong Wang**,[1,3] **and Jing Ma**[3]

[1]*Graduate School of Hebei Medical University, Shijiazhuang, China*
[2]*Hebei General Hospital, Shijiazhuang, China*
[3]*Hebei Key Laboratory of Reproductive Medicine, Hebei Reproductive Health Hospital, Shijiazhuang, China*

Correspondence should be addressed to Shusong Wang; wshsong@126.com and Jing Ma; mj5658700@126.com

Received 7 April 2023; Revised 6 August 2023; Accepted 18 December 2023; Published 16 January 2024

Academic Editor: Vikas Kumar Roy

Studies have reported the adverse effects of hyperuricemia on male reproduction, but the mechanism is still unclear. The purpose of this study is to explore the mechanism of hyperuricemia on reproductive system damage in male rats. The rats were divided into a control group and a model group. Rats were given hypoxanthine and potassium oxonate dissolved in 0.5% (*w*/*v*) sodium carboxymethyl cellulose solution to induce the hyperuricemia (HUA) model. After 6 weeks, the blood, testis, and epididymis tissues of the anesthetized rats were collected for further experiments and analysis. Compared with the control rats, the serum uric acid of HUA rats was significantly increased, and the serum testosterone, sperm count, and motility were significantly decreased. The protein expression of testosterone-related molecules CYP11A1, 3β-HSD, and StAR was downregulated in the testis of HUA rats. The protein expression of blood–testis barrier (BTB) related molecules ZO-1 and Connexin43 was downregulated in the testis of HUA rats. Compared with the control group, the zinc content and zinc-containing enzymes (ALP and LDH) were decreased, and the mRNA and protein expression of zinc transporters (ZnT4 and ZIP7) were downregulated in the testis of HUA rats. Furthermore, the level of MDA increased and the activities of CAT, GSH-PX, and SOD decreased in the testicular tissue of HUA rats. The PI3K/AKT/mTOR pathway in the testis of HUA rats was activated. However, there was no significant change in the protein expression of autophagy associated molecules LC3, Beclin1, and ATG5 in the testis of HUA rats. Thus, the conclusion is that hyperuricemia can lead to the destruction of BTB, impaired testosterone synthesis, and decreased sperm count and motility in male rats, mainly by inducing zinc homeostasis imbalance and oxidative stress, rather than autophagy.

1. Introduction

Hyperuricemia (HUA) is defined as the accumulation of excessive or insufficient excretion of serum uric acid (SUA) in the human body that causes serum uric acid to exceed normal levels [1]. The National Health and Nutrition Examination Survey (NHANES) from 2007 to 2008 showed that the total prevalence of hyperuricemia in American adults was 21.4% [2]. A recent systematic review found that the prevalence of hyperuricemia in Chinese increased from 8.5% to 18.4% from 2001 to 2017 [3]. Hyperuricemia closely related to the increased risk of metabolic syndrome, hypertension, type 2 diabetes, and cardiovascular disease [4–6]. It is worth noting that the average serum uric acid level in men is higher than that in women, which leads to the gender difference in the incidence of hyperuricemia [7]. The prevalence of hyperuricemia in men aged 20–29 years was twice that in women of the same age (21.5% vs. 8.9%) [3]. Therefore, we pay more attention to the impact of hyperuricemia on male health.

In fact, studies have confirmed that high uric acid levels have an adverse effect on male reproduction. The adverse effects of hyperuricemia on men are mainly reflected in erectile dysfunction, abnormal secretion of reproductive hormones, and decreased semen quality. Barassi et al. [8] found that uric acid levels were elevated in patients with arterial erectile dysfunction, and it was speculated that uric acid concentration could be used as a predictive risk factor for erectile dysfunction. Our previous studies have shown

that the imbalance of reproductive endocrine hormones, the increase of homocysteine concentration in seminal plasma, the decrease of organic acid content in seminal plasma, the decrease of antioxidant ability in seminal plasma, and the decrease of semen quality in patients with hyperuricemia [9]. Moreover, serum uric acid level is negatively correlated with the semen volume and total sperm count [10]. Furthermore, the mechanism of testicular injury in hyperuricemia rats was further explored at the microRNA level. It was found that the target mRNAs of differentially expressed microRNAs in the testis of hyperuricemia rats were rich in Wnt, Jak-STAT, mTOR, and MAPK signaling pathways [11]. However, the mechanism of testicular injury in hyperuricemia at mRNA and protein levels remains unclear. Therefore, this study established a hyperuricemia model and explored the molecular mechanism of testicular tissue damage in hyperuricemia male rats.

2. Materials and Methods

2.1. Animals and Model Establishment. Six-week-old male SD rats (SPF grade) were fed under standard conditions for 1 week and divided into control (CON) group ($n = 11$) and hyperuricemia (HUA) group ($n = 14$). The rats were given hypoxanthine (100 mg/kg) and potassium oxonate (250 mg/kg) dissolved in 0.5% (*w*/*v*) sodium carboxymethyl cellulose solution in the HUA group, and the control rats were given 0.5% (*w*/*v*) sodium carboxymethyl cellulose solution. After 6 weeks, the serum uric acid level was detected. The rats were then anesthetized and blood was collected. Bilateral epididymis and testis tissues were separated and weighed. All experimental procedures were approved by the ethics committee of Hebei Institute of Reproductive Health Science and Technology (animal ethics approval number: 2021-005).

2.2. Total Sperm Count and Sperm Motility. After the sperm was isolated from the epididymal tissue, the sperm suspension was dropped into the sperm counting plate, and total sperm count and sperm motility were counted under the optical microscope (LEICA DM750, Germany).

2.3. Detection of Serum Testosterone. The collected blood was centrifuged after coagulation to separate the serum. The serum testosterone values of the two groups were detected according to the instructions of ELISA kit. Serum testosterone was detected using an ELISA kit (Cayman Chemical Company, USA). SpectraMax® iD3 microplate reader (Shanghai Meigu Molecular Instrument Co., Ltd., China) was used to read the final result.

2.4. HE Staining. The paraffin sections were fixed with ice acetone for 5 min, and then washed with PBS three times, 5 min each time. Hematoxylin staining for 5 min. Put into the differentiation solution to differentiate for 1–2 s, rinse slowly with distilled water, and soak in the blue solution for 1 min. Dye in eosin staining solution for 2 min and rinse with distilled water. After staining, the sections were soaked in 85% ethanol for 1 min, 95% ethanol for 1 min, anhydrous Ethanol I and II for 5 min, transparent liquid I and II for 10 min, and finally sealed with neutral gum. The morphological structure of testicular tissue in the two groups was observed under the optical microscope (LEICA DM750, Germany). Johnson's [12] score was used to evaluate the histopathological damage of the testicular tissue sections.

2.5. Detection of Tatal Zinc Content in Testicular Tissue. We weighed 50 ± 5 mg of testicular tissue and added 1 mL of 65% nitric acid (guaranteed reagent, Merck) Microwave digestion until the solution is clear and transparent. After the solution was cooled, the ultrapure water was diluted to 10 mL. The final solution concentration was detected by inductively coupled plasma mass spectrometry (ICP-MS) (Agilent 7900C, USA).

2.6. Detection of Testicular Free Zinc. The frozen sections of testis were fixed in ice acetone for 10 min. After fixation, it was washed with PBS buffer for 5 min each time for three times. Zinquin Ethyl Ester solution (DOJINDO, Japan) was dropped on the testicular tissue and incubated in a wet box at 37°C for 2 hr. After incubation, sections were washed with PBS buffer at least three times for 5 min each time. Anti-fluorescence attenuation sealing agent (Beijing Solarbio Technology Co., Ltd.) was used for sealing. Zinc ion fluorescence was observed and images were collected in ImageXpress Micro Confocal (Molecular Devices, LLC, Sunnyvale, CA, USA).

2.7. Detection of Zinc-Containing Enzymes and Oxidative Stress Indicators. Each group of rats was weighed 50 mg of testicular tissue, and the protein was extracted using the specific extract of the kit. Protein concentration was detected by BCA kit (Generay Biotechnology, China). The levels of alkaline phosphatase (ALP), alcohol dehydrogenase (ADH; Nanjing Jiancheng, China). and lactate dehydrogenase (LDH) in testicular tissue were detected by kits (Beijing Box Biotechnology, China). The kit was used to detect glutathione peroxidase (GSH-PX; Nanjing Jiancheng, China), malondialdehyde (MDA), catalase (CAT), superoxide dismutase (SOD) (Beijing Box Biotechnology, China) in testicular tissue. SpectraMax® iD3 microplate reader (Shanghai Meigu Molecular Instrument, China) was used to read absorbance.

2.8. Quantitative Real-Time PCR (qRT-PCR). The gene expression of zinc transporter in testis tissues of different groups was detected by qRT-PCR. Total RNA was extracted from rat testicular tissue by animal total RNA extraction kit (Fuji, Chengdu, China) and subjected to reversely transcribed into cDNA using a Supersmart^{TM} 6 min 1st Strand cDNA Synthesis Kit (Zhongshi Gene, Tianjin, China) according to the instructions. The 20-μL qPCR reaction system included 1-μL cDNA, 0.4-μL forward primer, 0.4-μL reverse primer, 8.2-μL H_2O, and 10-μL 2 × SYBR Green Fast qPCR Mix (ABclonal, Wuhan, China). The sample Ct value was detected by a StepOnePlus real-time fluorescence quantitative PCR instrument (Applied Biosystems, Foster City, CA, USA). The primer sequences are listed in Table 1. The qPCR amplification program was set to 94°C for 3 min, 94°C for 15 s, and 60°C for 30 s for 40 cycles. The expression of the target gene was normalized to the expression of the GAPDH and calculated according to $2^{(Ct/_{GAPDH}\text{-}Ct/_{Gene\ of\ Interest})}$ [13].

Table 1: The sequences of the primers.

Gene	GeneBank	Sequence
Gapdh	NM_017008.4	F: 5′- ACTCTACCCACGGCAAGTTC-3′ R: 5′- TGGGTTTCCCGTTGATGACC-3′
Zip1	XM_006232707.2	F: 5′- GCCTTGGAGGCTCTTCATGT-3′ R: 5′- AAGCCAGTGTGATCTGCTCC-3′
Zip2	NM_001107260.1	F: 5′- ATGGTTCCAGACGGATGCAG-3′ R: 5′- TACTCCACGTAACTGGCAGC-3′
Zip3	NM_001008356.1	F: 5′- TGCATGGTGGGTGTGTTCTT-3′ R: 5′- AGCATGTAGCCAGGAAGACG-3′
Zip4	XM_008765563.2	F: 5′- AGCTCCATGCTACCCACAAC-3′ R: 5′- GGAGCTGCAGGCTTCACTTA-3′
Zip5	NM_001108728.1	F: 5′- CTGCATATGTGGGGGTGAGG-3′ R: 5′- CCCCAGAGCTCTCCTTAGGT-3′
Zip6	NM_001024745.1	F: 5′- GAAGGCGGAAATCCCTCCAA-3′ R: 5′- TAGGTTCTGAGCCGACAGGT-3′
Zip7	NM_001164744.1	F: 5′- CGATGCGTCTGCAACTCTTG-3′ R: 5′- TAACGGGGATGCCTCTCTCA-3′
Zip8	NM_001011952.1	F: 5′- AGGATCCACAGAAGCACAGC-3′ R: 5′- AAAGGGTCCCAATAGCCAGC-3′
Zip9	NXM_006240283.3	F: 5′- GCTGTAGTATTGGCGGCTCA-3′ R: 5′- AGAATGAGGGTGACACGACG-3′
Zip10	NM_001108796.2	F: 5′- CAATGAGTGGAGACGCCCTT-3′ R: 5′- AGCATCCGGTGTGCTGTTTA-3′
Zip11	NM_001013042.1	F: 5′- AAGCAGGAAGTGACTGTCGG-3′ R: 5′- CATGACCCCTGCAGCAAAAC-3′
Zip12	NM_001106124.1	F: 5′- ATTGGTCTCTCGGTGTCTGC-3′ R: 5′- GAAGCATCCCCACCAAGGAT-3′
Zip13	XM_006234502.3	F: 5′- TGTACGCAATCCCCCAAAGG-3′ R: 5′- GTAGCACATTCACCAGGGCA-3′
Zip14	NM_001107275.1	F: 5′- CTCCCCACTCTTGCCTCTTG-3′ R: 5′- GGACCCTAAGCCTACCAGGA-3′
ZnT1	NM_022853.2	F: 5′- AGAGCTGATGAACAGCACCC-3′ R: 5′- AGCTGCCAGACGTGTAACTC-3′
ZnT2	NM_001083122.1	F: 5′- AATGGGGGAGCGGGTTAAAG-3′ R: 5′- GGTCACTCATGGTTCCCTGG-3′
ZnT3	NM_001013243.1	F: 5′- CTGGATAGTCACCGGCATCC-3′ R: 5′- TACTCTGCACCCCTAGGTCC-3′
ZnT4	NM_172066.1	F: 5′- ACTTGTGGCATTCACAACGC-3′ R: 5′- TTTCGACTGCACTTCCTCCC-3′
ZnT5	NM_001106404.1	F: 5′- ATTTTTGGCGCCATTCTGCC-3′ R: 5′- TTATCCACCTCCACTGTTCACG-3′
ZnT6	NM_001277279.1	F: 5′- CTTGTGCGGCATTATCCCAG-3′ R: 5′- ACACCCCATCCAAGGTAGAC-3′
ZnT7	NM_001191715.1	F: 5′- TGCTTCCCCAGTGCTATCAG-3′ R: 5′- GCACTGGGTAGTACAATGCC-3′
ZnT8	NM_001130538.1	F: 5′- GCACTGATGTAGGACGCACT-3′ R: 5′- CAGGCTTCTGTCCACGTTCT-3′
ZnT9	NM_001109088.1	F: 5′- GAAAGGTGGTGATGGTCGCT-3′ R: 5′- ACGGGTGAGAAGGATCTGGT-3′
ZnT10	NM_001105985.1	F: 5′- TCAGCGGGCTGTAAAGATGG-3′ R: 5′- GTTGAACGAGTCCGAGAGCA-3′

Gapdh, glyceraldehyde-3-phosphate dehydrogenase; *Zip1 (SLC39A1)*, Zrt-Irt-like protein 1; *Zip2 (SLC39A2)*, Zrt-Irt-like protein 2; *Zip3 (SLC39A3)*, Zrt-Irt-like protein 3; *Zip4 (SLC39A4)*, Zrt-Irt-like protein 4; *Zip5 (SLC39A5)*, Zrt-Irt-like protein 5; *Zip6 (SLC39A6)*, Zrt-Irt-like protein 6; *Zip7 (SLC39A7)*, Zrt-Irt-like protein 7; *Zip8 (SLC39A8)*, Zrt-Irt-like protein 8; *Zip9 (SLC39A9)*, Zrt-Irt-like protein 9; *Zip10 (SLC39A10)*, Zrt-Irt-like protein 10; *Zip11 (SLC39A11)*, Zrt-Irt-like protein 11; *Zip12 (SLC39A12)*, Zrt-Irt-like protein 12; *Zip13 (SLC39A13)*, Zrt-Irt-like protein 13; *ZIP14 (SLC39A14)*, Zrt-Irt-like protein 14; *ZnT1 (SLC30A1)*, zinc transporter 1; *ZnT2 (SLC30A2)*, zinc transporter 2; *ZnT3 (SLC30A3)*, zinc transporter 3; *ZnT4 (SLC30A4)*, zinc transporter 4; *ZnT5 (SLC30A5)*, zinc transporter 5; *ZnT6 (SLC30A6)*, zinc transporter 6; *ZnT7 (SLC30A7)*, zinc transporter 7; *ZnT8 (SLC30A8)*, zinc transporter 8; *ZnT9 (SLC30A9)*, zinc transporter 9; *ZnT10 (SLC30A10)*, zinc transporter 10.

Table 2: Source of the first antibody.

Antibody	Source	Dilution	Catalog	Company
Anti-GAPDH	Mouse mAb	1 : 5,000	YM3029	Immunoway
Anti-ZnT4	Rabbit pAb	1 : 1,000	DF4633	Affinity
Anti-ZIP7	Rabbit pAb	1 : 2,000	ab254566	Abcam
Anti-3β-HSD	Rabbit mAb	1 : 1,000	A19266	ABclonal
Anti-StAR	Mouse mAb	1 : 200	sc-166821	Santa Cruz
Anti-CYP11A1	Rabbit pAb	1 : 1,000	13363-1-AP	Proteintech
Anti-ZO-1	Rabbit pAb	1 : 1,000	GTX108613	GeneTex
Anti- Connexin43	Mouse mAb	1 : 1,000	610061	BD Biosciences
Anti-Occludin	Rabbit pAb	1 : 1,000	R1510-33	HUABIO
Anti-β-catenin	Rabbit mAb	1 : 1,000	ET1601-5	HUABIO
Anti-N-cadherin	Rabbit pAb	1 : 1,000	GTX127345	GeneTex
Anti-ATG5	Rabbit mAb	1 : 1,000	ET1611-38	HUABIO
Anti-LC3	Rabbit pAb	1 : 500	14600-1-AP	Proteintech
Anti-Beclin1	Rabbit pAb	1 : 1,000	PD017	MBL
Anti-PI3K	Rabbit pAb	1 : 500	A0265	ABclonal
Anti-p-PI3K	Rabbit pAb	1 : 1,000	#4292	CST
Anti-AKT	Rabbit mAb	1 : 1,000	ET1609-51	HUABIO
Anti-p-AKT	Rabbit mAb	1 : 1,000	#4060	CST
Anti-mTOR	Mouse mAb	1 : 2,500	66888-1-Ig	Proteintech
Anti-p-mTOR	Mouse mAb	1 : 2,500	67778-1-Ig	Proteintech

AKT, protein kinase B; ATG5, autophagy-related 5; Beclin1, bcl-2-interacting protein 1; CYP11A1, cytochrome P45011A1 enzyme; GAPDH, glyceraldehy-3-phosphate dehydrogenase; 3β-HSD, 3β-Hydroxysteroid dehydrogenase/isomerase; LC3, light chain 3; mTOR, mammalian target of rapamycin; PI3K, phosphoinositide 3-kinase; p-PI3K (p85), phosphorylated PI3K; p-AKT (Ser473), phosphorylated AKT; p-mTOR (Ser2448), phosphorylated mTOR; StAR, steroidogenic acute regulatory protein; ZIP7, zrt-Irt-like protein 7; ZnT4, zinc transporter 4; ZO-1, Zonula, Zonula Occludens-1.

2.9. Western Blotting. Rat testicular tissue was fully lysed with RIPA lysate (Solarbio Biotech Co., China) and protein concentration was measured with BCA kit (Generay Biotechnology, China). The same amount of protein samples was separated by SDS-PAGE and transferred to PVDF membrane (Sigma, USA) by wet transfer method. The PVDF membrane was blocked with 5% skim milk for 2 hr. The primary antibody was incubated overnight at 4°C. The use of primary antibody is shown in Table 2. The membrane was placed on a shaker and washed three times with 1 × TBST solution for 10 min each time and was incubated in secondary antibody for 1.5 hr at room temperature. Goat anti-rabbit or goat anti-mouse were purchased from Selacare Biotechnology (USA). After incubation, the membrane was washed with 1 × TBST solution for three times and 1 × TBS solution for one time, 10 min each time. The strips were soaked in ultrasensitive ECL chemiluminescence detection reagent (Shanghai Liji Biological, China) and detected by chemiluminescence imager (MinioChemi320, Sage Creation Science Company, Beijing, China). Image J 1.8.0 software (National Institutes of Health) was used for data analysis. Each group of samples were repeated at least three times to take the average.

2.10. Data Analysis. Measurement data conforming to normal distribution were expressed as mean ± standard deviation (M ± SD). *T*-test was used for comparison between the two groups. $P < 0.05$ indicated that the difference was statistically significant. GraphPad Prism software (version 8.0.1) was used to analyze data results and draw pictures.

3. Results

3.1. Establishment of Hyperuricemia Model and Its Effect on Testicular Tissue. The serum uric acid of rats in HUA group increased significantly ($P < 0.01$; Figure 1(a)). To study the effect of elevated serum uric acid on the reproduction of male rats, we measured the weight of testis, serum testosterone, sperm count, and sperm motility. There was no difference in testicular weight between the two groups ($P > 0.05$; Figure 1(b)). Serum testosterone in HUA rats was significantly lower than that in the CON rats ($P < 0.05$; Figure 1(c)). Compared with the CON group, the sperm count and sperm motility in HUA rats were significantly decreased ($P < 0.05$; Figures 1(d) and 1(e)). HE staining showed that the seminiferous tubules in the testis of rats in CON group were arranged neatly, and there were spermatogenic cells in the lumen at all stages of development, and the Sertoli cells and Leydig cells were arranged densely and structurally intact. However, in HUA group, the arrangement of spermatogenic tubules was disordered, the basal structure of tubules was incomplete, the lumen was enlarged, vacuoles increased, and spermatogenic cells at all levels, Sertoli cells and Leydig cells decreased significantly (Figure 1(f)). The Johnson's score was significantly decreased in HUA groups compared with the CON group ($P < 0.0001$; Table 3).

3.2. Hyperuricemia Caused Testosterone Synthesis Disorder. The protein expression of testosterone synthesis protein 3βHSD, CYP11A1, and StAR in the testicular tissue of HUA group decreased ($P < 0.05$; Figure 2).

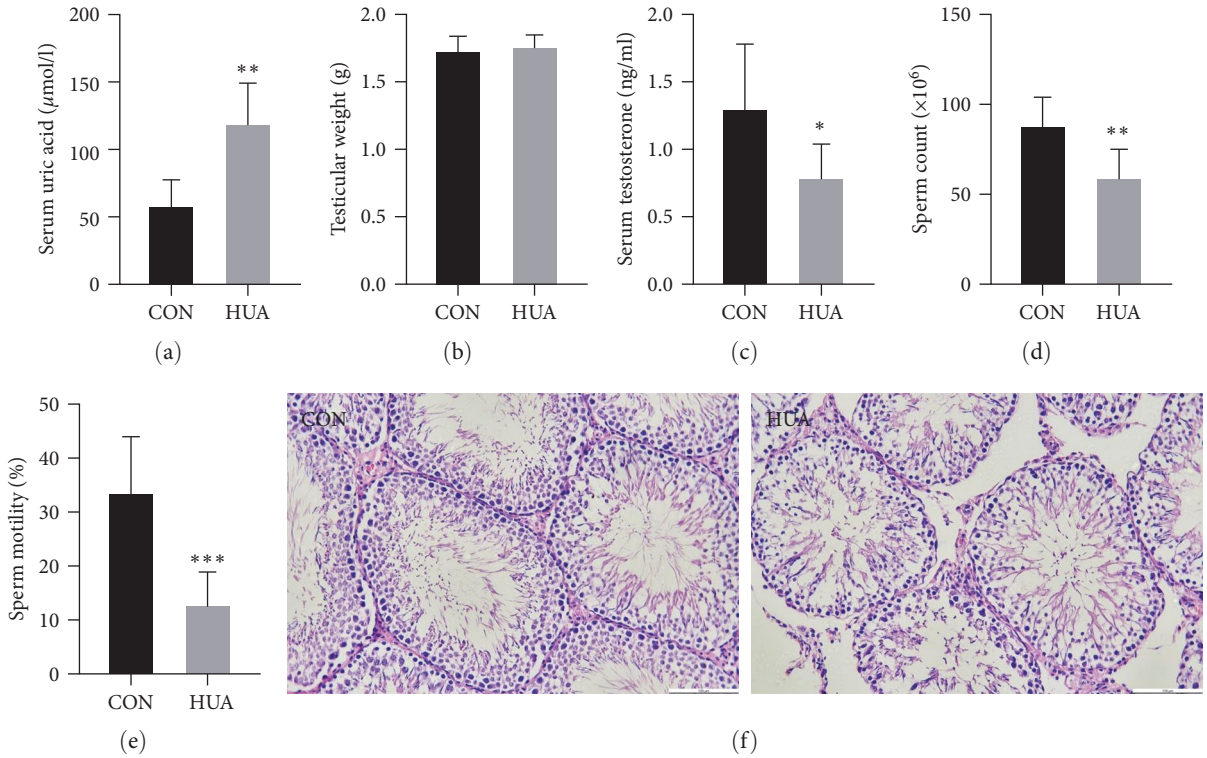

Figure 1: The basic situation of hyperuricemia rats. (a) The serum uric acid, (b) testicular weight, (c) serum testosterone, (d) sperm count, and (e) sperm motility of rats in CON and HUA groups. (f) HE staining results of testis tissues (scale bar: 100 μm). CON, control; HUA, hyperuricemia. $^{*}P<0.05$; $^{**}P<0.01$; $^{***}P<0.001$; compared with CON group.

Table 3: Johnson's score of the two groups.

—	Control group	Hyperuricemia group	P
Johnson's score	8.99 ± 0.69	5.84 ± 1.14	<0.0001

3.3. Hyperuricemia Destroyed the Blood–Testis Barrier. The expression of tight junction protein ZO-1 protein in HUA rats was decreased, and the expression of gap junction protein Connexin43 protein was significantly decreased ($P<0.05$; Figure 3).

3.4. Comparison of Zinc Homeostasis in Testicular Tissue. ICP-MS results showed that the zinc content in the testis of HUA group decreased ($P<0.05$; Figure 4(a)). Zinquin ethyl ester showed that the free zinc concentration in testicular tissue of HUA group decreased (Figure 4(e)). The levels of ALP and LDH in HUA group were lower than those in the control group ($P<0.05$), and there was no change in ADH ($P>0.05$; Figure 4(b)–4(d)).

The results of qRT-PCR showed that the most significant change in Zip family mRNAs in the two groups was Zip7. The most significant change and high expression of ZnT family mRNAs is ZnT4. Compared with CON group, the mRNA expression of Zip7 and ZnT4 in the testis of rats in HUA group was decreased (Figures 4(f) and 4(g)). Western blotting results showed that the protein expression of zinc transporter ZIP7 and ZnT4 in testis tissue of HUA rats decreased ($P<0.01$; Figure 4(h)).

3.5. Changes of Oxidative Stress Level in Testicular Tissue. Compared with CON group, the level of oxidative stress in testis of HUA group increased, the activity of SOD and GSH-PX decreased, and the level of MDA increased ($P<0.05$; Figure 5).

3.6. The PI3K/AKT/mTOR Pathway Was Activated in HUA Rats. Compared with the CON group, there was no significant change in the protein expression of PI3K, AKT, and mTOR ($P>0.05$), and the protein expression of p-PI3K, p-AKT, and p-mTOR was significantly increased in HUA group ($P<0.05$; Figure 6). The results showed that the PI3K/AKT/mTOR pathway was activated in the testicular tissue of HUA rats.

3.7. The Level of Autophagy in Hyperuricemia Testis Did Not Change. Compared with CON group, there was no difference in the protein expression of LC3, Beclin1, and ATG5 in the testis tissue of HUA group ($P>0.05$; Figure 7), indicating that the level of autophagy did not change.

4. Discussion

Uric acid is an independent factor affecting semen volume and total sperm count [10]. It is found that hyperuricemia can cause purine metabolism disorder and male androgen homeostasis imbalance [14]. Usually, hyperuricemia models are established by intraperitoneal injection or oral administration of uric acid and its analogs or uricase inhibitor potassium oxonate [15, 16]. We observed a significant increase in serum uric acid levels in the model group by intragastric

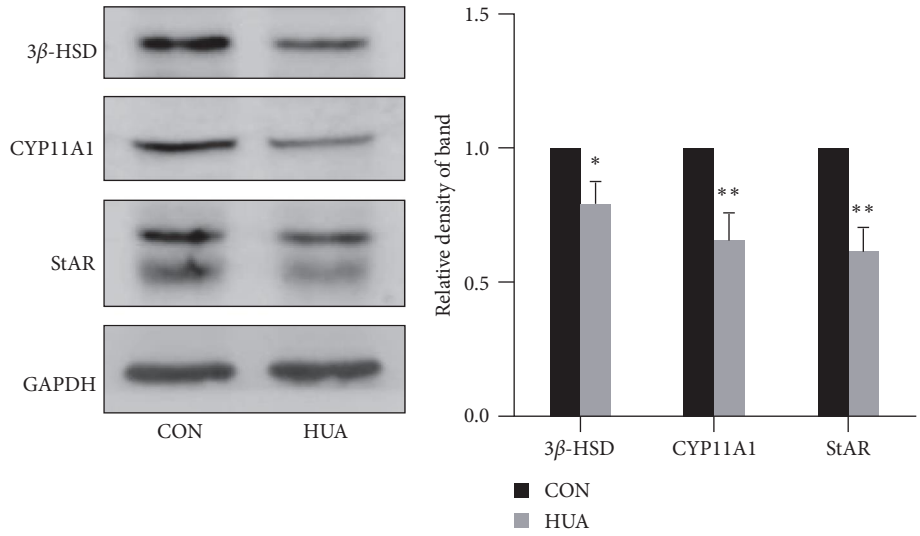

Figure 2: Testosterone synthesis disorder in testis tissue of hyperuricemia rats. (a) Protein expression views and (b) densitrometric quantification analysis of 3β-HSD, CYP11A1 and StAR. 3β-HSD, 3β-Hydroxysteroid dehydrogenase/isomerase; CYP11A1, cytochrome P45011A1 enzyme; GAPDH, glyceraldehy-3-phosphate dehydrogenase; StAR, steroidogenic acute regulatory protein. $^{*}P<0.05$; $^{**}P<0.01$; compared with CON group.

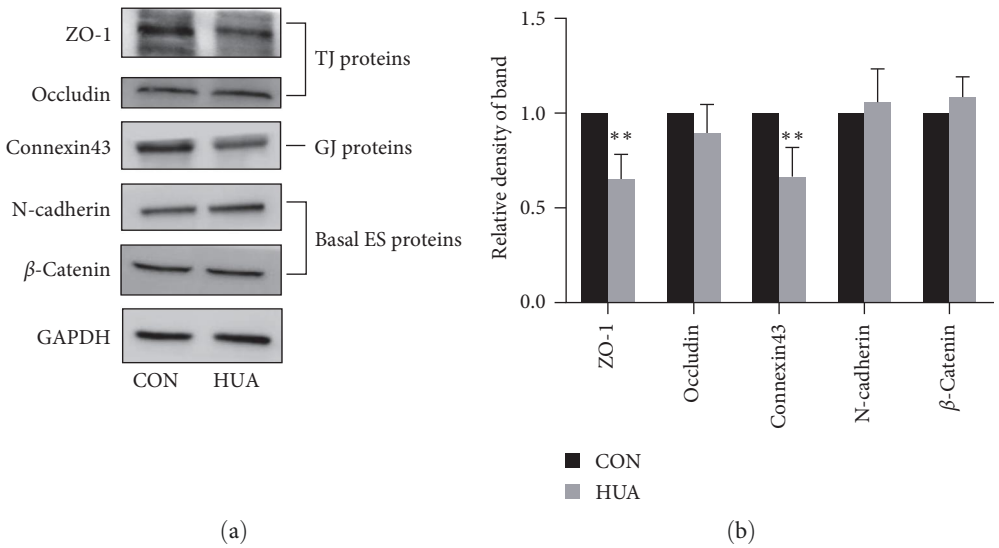

Figure 3: Destruction of blood-testis barrier in testis tissue of hyperuricemia rats. (a) Protein expression views and (b) densitrometric quantification analysis of ZO-1, Occludin, Connexin43, N-ccadherin, and β-catenin. ZO-1, Zonula Occludens-1. $^{**}P<0.01$; compared with CON group.

administration of 100 mg/kg hypoxanthine and 250 mg/kg potassium oxonate for 6 weeks. We have successfully constructed a hyperuricemia model and found that hyperuricemia can lead to testicular structural damage, decreased serum testosterone, sperm count, and motility in male rats.

Testosterone is an essential steroid hormone for male growth and development, maintenance of secondary sexual characteristics, and promotion of sperm maturation and release [17]. There are many enzymes involved in the process of testosterone synthesis, and many factors affect testosterone levels by affecting enzyme activity [18]. Our previous studies have confirmed that serum testosterone decreased in hyperuricemia men compared with control group, suggesting the negative impact of hyperuricemia on reproductive hormones [19]. The present study found that compared with the control group, the expression of testosterone synthesis proteins CYP11A1, 3β-HSD, and StAR in the testis of the model group decreased, resulting in a negative regulation of the testosterone synthesis process and a decrease in testosterone levels.

Testosterone can also provide a favorable environment for germ cell development by maintaining the integrity of the blood–testis barrier (BTB) [20]. The BTB divides spermatogenic

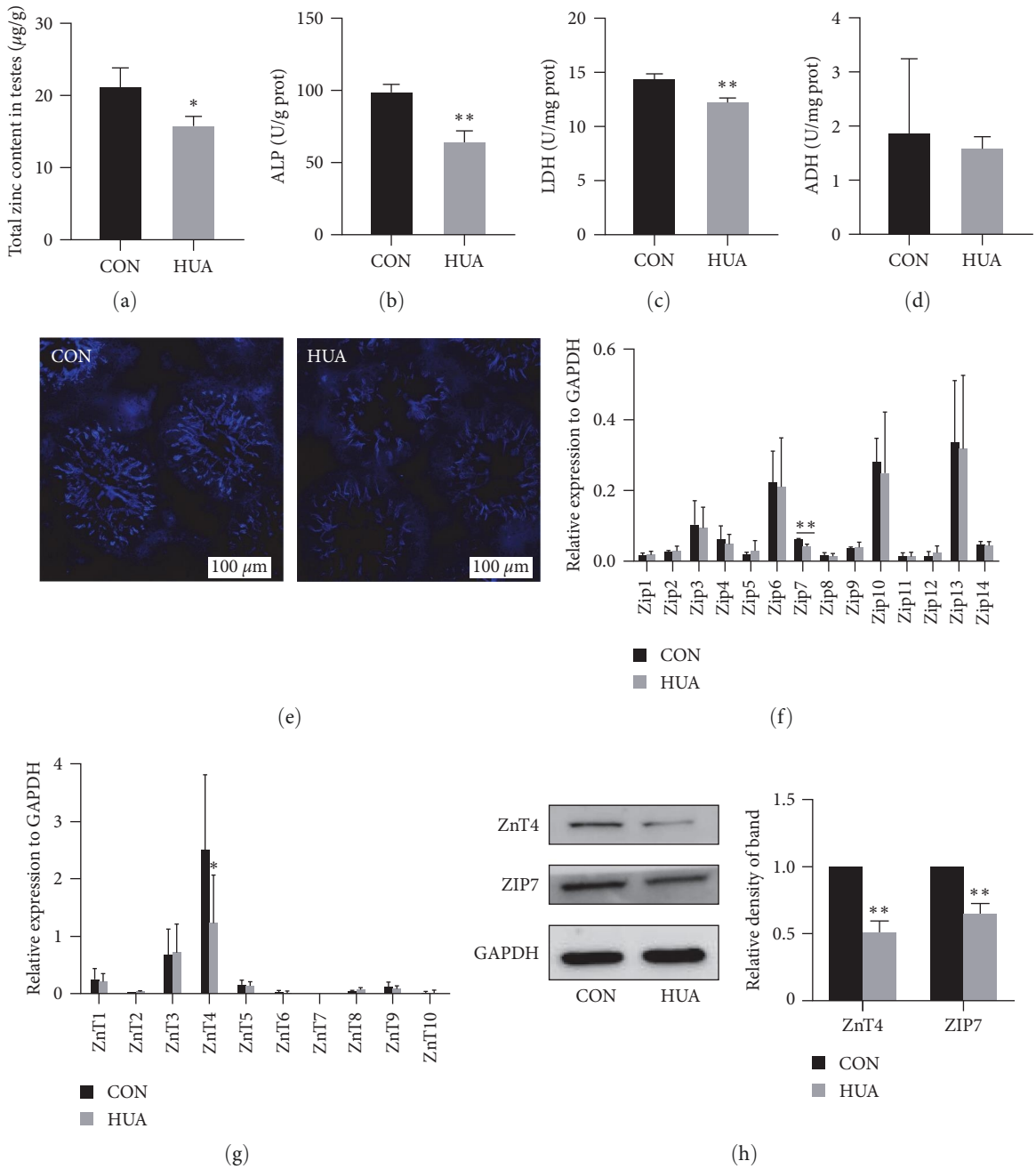

FIGURE 4: Imbalance of zinc homeostasis in testis of hyperuricemia rats. (a) Total zinc content in testis tissues. The content of zinc metalloenzyme (b) ALP, (c) LDH and (d) ADH in testis tissues. (e) Zinquin ethyl ester probe staining to test free zinc in testicular tissue (Scale bar: 100 μm). Transcriptional level of (f) ZIP family and (g) ZnT family genes examined by qPCR assay. (h) Protein expression views and densitrometric quantification analysis of ZnT4 and ZIP7. GAPDH, glyceraldehy-3-phosphate dehydrogenase; ZIP, zrt-Irt-like protein; ZIP7, zrt-Irt-like protein 7; ZnT, zinc transporter; ZnT4, zinc transporter 4. $^{*}P<0.05$; $^{**}P<0.01$; compared with CON group.

epithelium into basal chamber and inner chamber, which creates microenvironment for meiosis and development of spermatids into spermatozoa [21]. BTB in mammalian testis is composed of tight junction (TJ), basal ectoplasmic specialization (basal ES), gap junction (GJ), and desmosomes [22]. We detected the protein levels of tight junction proteins ZO-1 and Occludin, basic ES proteins β-catenin and N-Cadherin, and GJ protein Connexin43 in the testicular tissues of the two groups of rats. The results showed that the protein expression of ZO-1 and Connexin43 decreased, and the protein expression of occludin, β-catenin, and N-Cadherin did not change, indicating that hyperuricemia mainly induced the destruction of the BTB barrier by affecting TJ and GJ. The destruction of BTB further impairs spermatogenesis, thus reducing semen quality.

As an important trace element in human body, zinc is involved in the development of male reproductive system, the regulation of androgen level, spermatogenesis, sperm quality, and fertilization [23]. Zinc is closely related to the

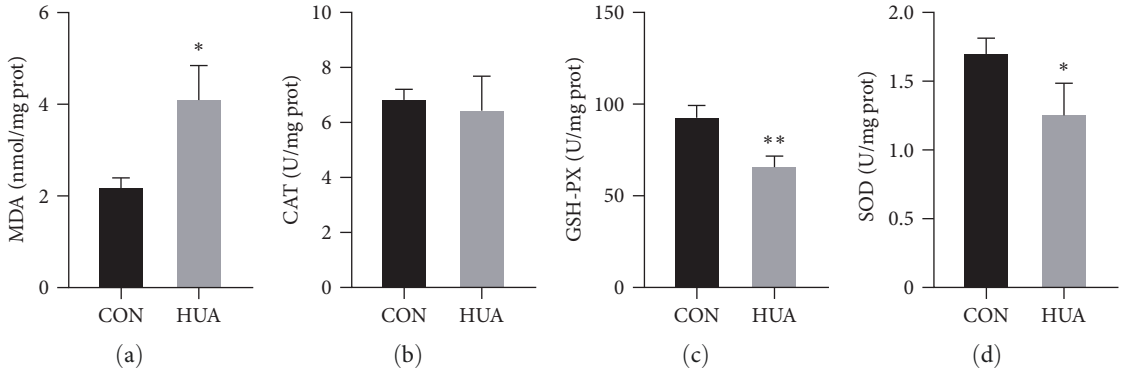

Figure 5: Increased oxidative stress in the testis of rats with hyperuricemia. Contents of (a) MDA and activities of (b) CAT, (c) GSH-PX, and (d) SOD in testis tissues. CAT, catalase; GSH-PX, glutathione peroxidase; MDA, malondialdehyde; SOD, superoxide dismutase. $^{*}P<0.05$; $^{**}P<0.01$; compared with CON group.

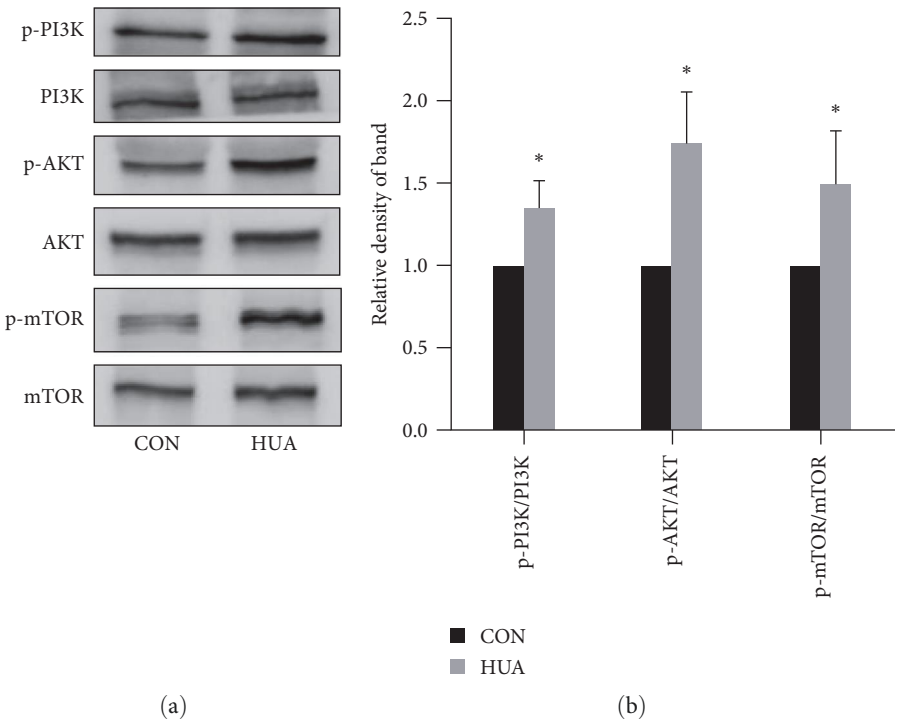

Figure 6: Activated PI3K/AKT/mTOR pathway in testis tissue of hyperuricemia rats. (a) Protein expression views and (b) densitometric quantification analysis of p-PI3K, PI3K, p-AKT, AKT, p-mTOR, and mTOR. AKT, protein kinase B; GAPDH, glyceraldehy-3-phosphate dehydrogenase; mTOR, mammalian target of rapamycin; PI3K, phosphoinositide 3-kinase; p-PI3K (p85), phosphorylated PI3K; p-AKT (Ser473), phosphorylated AKT; p-mTOR (Ser2448), phosphorylated mTOR. $^{*}P<0.05$; compared with CON group.

testosterone synthesis. Our recently published systematic review summarized that zinc deficiency will lead to the decrease of serum total testosterone, and proper zinc supplementation can positively regulate steroid hormone synthesis genes and thus increases testosterone levels [24]. Therefore, we examined zinc content and related indicators to observe whether zinc homeostasis is involved in testicular injury in hyperuricemic rats. Zinc plays an important role in the structure and function of many enzymes, including ALP, LDH, and ADH [25, 26]. In this study, it was observed that the zinc, free zinc concentration, ALP, and LDH content in testis of HUA group decreased, and ADH level did not change significantly. In fact, the regulation of cellular zinc levels mainly relies on zinc transporters to transport zinc ions across the membrane [27]. The zinc transporter family mainly includes ZnT and ZIP families [28]. The ZnT family mainly transfer zinc ions from the cytoplasm to the extracellular (including organelles), and the ZIP family transport extracellular (including organelles) zinc ions into the cytoplasm [29]. Our results showed that Zip7 and ZnT4 are the two transporters with the most obvious changes in mRNA and protein expression. ZnT4 is located in the trans-Golgi network (TGN) and cell membrane, providing zinc ions to zinc-dependent proteins in the TGN, which is essential for normal cell function and zinc output [30]. Prostate epithelial cells can store zinc ions into lysosomes through ZnT4 when exposed to high glucose, thereby

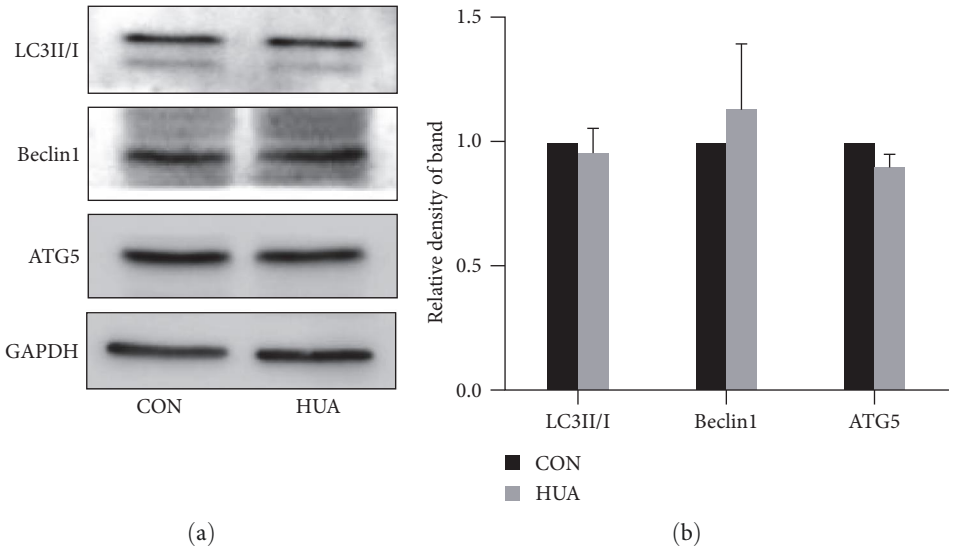

Figure 7: The level of autophagy in the testis of hyperuricemia rats did not change. (a) Protein expression views and (b) densitrometric quantification analysis of LC3II/I, Beclin1, and ATG5. ATG5, autophagy-related 5; Beclin1, bcl-2-interacting protein 1; GAPDH, glyceraldehy-3-phosphate dehydrogenase; LC3, light chain 3.

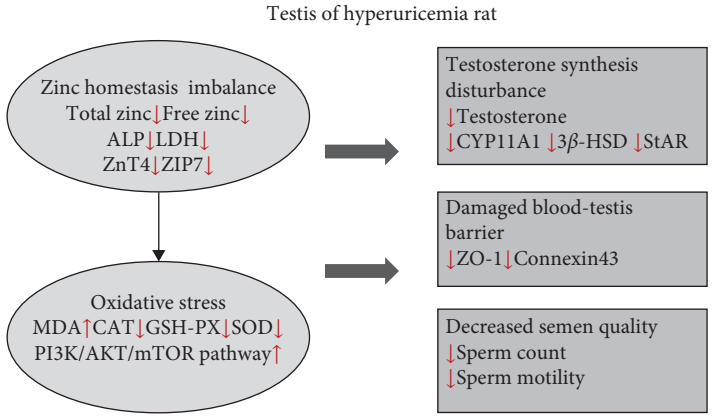

Figure 8: The effect of hyperuricemia-induced reproductive injury in male rats and the summary of this study.

regulating zinc homeostasis [31]. ZIP7 is widely expressed in a variety of tissues, and is located in the endoplasmic reticulum [32]. It can transport zinc ions in the endoplasmic reticulum to the cytoplasm, thus affecting intracellular signal transduction and normal cell function [33]. The content of ZIP7 in rat pachytene spermatocytes was almost 3.5 times that in round sperm cells, suggesting that ZIP7 may be involved in the regulation of zinc homeostasis during spermatogenesis [34]. Our results showed that the mRNA and protein expression of ZnT4 and ZIP7 in the testis of HUA rats were decreased, and the zinc transport function was disordered, which caused the levels of zinc enzyme, total zinc and free zinc were decreased. Thus, we speculate that the decrease of zinc transporter expression in testis of HUA rats affects normal zinc transport and causes the destruction of zinc homeostasis.

Zinc has been shown to have antioxidant properties, and decreased zinc concentration can lead to DNA damage, increased protein and lipid oxidation [23, 35]. Recent studies have shown that elevated reactive oxygen species (ROS) levels and oxidative stress caused by zinc deficiency are one of the important causes of poor sperm quality and male infertility [23]. Hyperuricemia was closely related to the production of ROS [36]. Several studies have demonstrated that hyperuricemia causes a variety of diseases by activating oxidative stress [37–39]. In order to explore the potential mechanism of testosterone reduction and BTB damage, we examined the activity of SOD, GSH-PX, CAT, and MDA in testicular tissue. Our results showed that the activity of SOD and GSH-PX in the testicular tissue of HUA rats was lower than that of CON group, and the level of MDA was higher than that of CON group, indicating that the level of oxidative stress in the tissue was increased. The results showed that oxidative stress is involved in the process of reproductive injury in hyperuricemia rats. Moreover, oxidative stress may be caused by zinc homeostasis imbalance in testicular tissue.

The phosphoinositide 3-kinase (PI3K)/protein kinase B (AKT)/mammalian target of rapamycin (mTOR) signaling pathway is involved in many stages of male reproduction, including

the regulation of the hypothalamic–pituitary–gonad (HPG) axis during spermatogenesis, the proliferation and differentiation of spermatogonia and testicular cells [40]. Uric acid can mediate oxidative stress and autophagy by activating PI3K/AKT/mTOR pathway. Uric acid has been proved to lead to the production of mitochondrial ROS by activating mTOR [41]. Uric acid can phosphorylate Akt and activate mTOR, which blocks autophagy and promotes inflammation through hypoxia-inducible factor (HIF)-1α [42, 43]. We examined the protein expression of PI3K, p-PI3K, AKT, p-AKT, mTOR, and p-mTOR. The results showed that hyperuricemia promoted the phosphorylation of PI3K and further activated the phosphorylation of downstream effector molecule AKT. AKT activated mTOR and increased the level of phosphorylated mTOR, indicating that PI3K/AKT/mTOR pathway may be activated by oxidative stress. The PI3K/AKT/mTOR pathway is involved in the regulation of autophagy, so we also detected the protein levels of autophagy-related proteins LC3, ATG5, and Beclin1 [44]. Interestingly, no changes in autophagy levels were observed in this study.

5. Conclusion

Collectively, we found the damaged testis structure, testosterone synthesis disorder and the decreased sperm count and sperm motility in hyperuricemia rats. Our results showed that in testicular tissue of hyperuricemia rats the zinc homeostasis was imbalanced and the level of oxidative stress was increased, but autophagy levels were not changed (Figure 8). Therefore, zinc homeostasis and oxidative stress may be important events in hyperuricemia affecting male reproduction.

Data Availability

The original contributions presented in the study are included in the article. Further inquiries can be directed to the corresponding author.

Conflicts of Interest

The authors declare that the research was conducted in the absence of any commercial or financial relationships that could be construed as a potential conflicts of interest.

Authors' Contributions

Liger Te, Shusong Wang, and Jing Ma conceived and designed the experiments. Liger Te, Yuejia Li, and Junsheng Liu performed the experiments. Xuan Liu and Ming Zhao analyzed the data and prepared all the figures. Liger Te wrote the original draft. Shusong Wang and Jing Ma revised the manuscript. All authors read and approved the final version of the manuscript.

Acknowledgments

This study was sponsored by Hebei Natural Science Foundation (grant nos. H2021314001 and H2022314001) and S&T Program of Hebei (grant no. 226Z7722G).

References

[1] N. L. Edwards, "The role of hyperuricemia in vascular disorders," *Current Opinion in Rheumatology*, vol. 21, no. 2, pp. 132–137, 2009.

[2] Y. Zhu, B. J. Pandya, and H. K. Choi, "Prevalence of gout and hyperuricemia in the US general population: the National Health and Nutrition Examination Survey 2007–2008," *Arthritis & Rheumatism*, vol. 63, no. 10, pp. 3136–3141, 2011.

[3] Y. Li, Z. Shen, B. Zhu, H. Zhang, X. Zhang, and X. Ding, "Demographic, regional and temporal trends of hyperuricemia epidemics in mainland China from 2000 to 2019: a systematic review and meta-analysis," *Global Health Action*, vol. 14, no. 1, Article ID 1874652, 2021.

[4] H.-L. Sun, D. Pei, K.-H. Lue, Y.-L. Chen, and S. Kaser, "Uric acid levels can predict metabolic syndrome and hypertension in adolescents: a 10-year longitudinal study," *PLOS ONE*, vol. 10, no. 11, Article ID e0143786, 2015.

[5] I. Sluijs, J. W. J. Beulens, D. L. van der A, A. M. W. Spijkerman, M. B. Schulze, and Y. T. van der Schouw, "Plasma uric acid is associated with increased risk of type 2 diabetes independent of diet and metabolic risk factors," *The Journal of Nutrition*, vol. 143, no. 1, pp. 80–85, 2013.

[6] T. Okura, J. Higaki, M. Kurata et al., "Elevated serum uric acid is an independent predictor for cardiovascular events in patients with severe coronary artery stenosis subanalysis of the Japanese Coronary Artery Disease (JCAD) study," *Circulation Journal*, vol. 73, no. 5, pp. 885–891, 2009.

[7] S. Copur, A. Demiray, and M. Kanbay, "Uric acid in metabolic syndrome: does uric acid have a definitive role?" *European Journal of Internal Medicine*, vol. 103, pp. 4–12, 2022.

[8] A. Barassi, M. M. Corsi Romanelli, R. Pezzilli et al., "Levels of uric acid in erectile dysfunction of different aetiology," *The Aging Male*, vol. 21, no. 3, pp. 200–205, 2018.

[9] T. Cui, Y.-W. Gong, J. Ma, R.-Y. Han, and S.-S. Wang, "Establishment of a method for detection of thiols in seminal plasma and its application in patients with hyperuricemia," *Zhonghua Nan Ke Xue*, vol. 27, no. 7, pp. 603–608, 2021.

[10] R.-Y. Han, J. Ma, T. Cui et al., "Hyperuricemia reduces semen parameters in infertile men," *Zhonghua Nan Ke Xue*, vol. 24, no. 12, pp. 1069–1072, 2018.

[11] H. Sung, J. Ferlay, R. L. Siegel et al., "Global cancer statistics 2020: GLOBOCAN estimates of incidence and mortality worldwide for 36 cancers in 185 Countries," *CA: A Cancer Journal for Clinicians*, vol. 71, no. 3, pp. 209–249, 2021.

[12] S. G. Johnsen, "Testicular biopsy score count—a method for registration of spermatogenesis in human testes: normal values and results in 335 hypogonadal males," *Hormones*, vol. 1, no. 1, pp. 2–25, 1970.

[13] J. Yang, Y. Zhang, X. Cui et al., "Gene profile identifies zinc transporters differentially expressed in normal human organs and human pancreatic cancer," *Current Molecular Medicine*, vol. 13, no. 3, pp. 401–409, 2013.

[14] I. V. Mukhin, G. A. Ignatenko, and V. Y. Nikolenko, "Dyshormonal disorders in gout: experimental and clinical studies," *Bulletin of Experimental Biology and Medicine*, vol. 133, no. 5, pp. 491–493, 2002.

[15] R. Dhouibi, H. Affes, M. B. Salem et al., "Creation of an adequate animal model of hyperuricemia (acute and chronic hyperuricemia); study of its reversibility and its maintenance," *Life Sciences*, vol. 268, Article ID 118998, 2021.

[16] K. Nishizawa, N. Yoda, F. Morokado et al., "Changes of drug pharmacokinetics mediated by downregulation of kidney organic cation transporters Mate1 and Oct2 in a rat model of

hyperuricemia," *PLOS ONE*, vol. 14, no. 4, Article ID e0214862, 2019.

[17] W. H. Walker, "Androgen actions in the testis and the regulation of spermatogenesis," in *Molecular Mechanisms in Spermatogenesis*, C. Cheng and F. Sun, Eds., vol. 1381 of *Advances in Experimental Medicine and Biology*, pp. 175–203, Springer, Cham, 2021.

[18] R. S. Ge, X. Li, and Y. Wang, "Leydig cell and spermatogenesis," in *Molecular Mechanisms in Spermatogenesis*, C. Cheng and F. Sun, Eds., vol. 1381 of *Advances in Experimental Medicine and Biology*, pp. 111–129, Springer, Cham, 2021.

[19] J. Ma, R. Han, T. Cui, C. Yang, and S. Wang, "Effects of high serum uric acid levels on oxidative stress levels and semen parameters in male infertile patients," *Medicine*, vol. 101, no. 3, Article ID e28442, 2022.

[20] L. B. Smith and W. H. Walker, "The regulation of spermatogenesis by androgens," *Seminars in Cell & Developmental Biology*, vol. 30, pp. 2–13, 2014.

[21] D. D. Mruk and C. Y. Cheng, "The mammalian blood–testis barrier: its biology and regulation," *Endocrine Reviews*, vol. 36, no. 5, pp. 564–591, 2015.

[22] C. Y. Cheng, D. D. Mruk, and D. R. Sibley, "The blood–testis barrier and its implications for male contraception," *Pharmacological Reviews*, vol. 64, no. 1, pp. 16–64, 2012.

[23] A. Fallah, A. Mohammad-Hasani, and A. H. Colagar, "Zinc is an essential element for male fertility: a review of Zn roles in men's health, germination, sperm quality, and fertilization," *Journal of Reproduction & Infertility*, vol. 19, no. 2, pp. 69–81, 2018.

[24] L. Te, J. Liu, J. Ma, and S. Wang, "Correlation between serum zinc and testosterone: a systematic review," *Journal of Trace Elements in Medicine and Biology*, vol. 76, Article ID 127124, 2023.

[25] T. Kambe, T. Tsuji, A. Hashimoto, and N. Itsumura, "The physiological, biochemical, and molecular roles of zinc transporters in zinc homeostasis and metabolism," *Physiological Reviews*, vol. 95, no. 3, pp. 749–784, 2015.

[26] D. S. Auld and T. Bergman, "Medium- and short-chain dehydrogenase/reductase gene and protein families: the role of zinc for alcohol dehydrogenase structure and function," *Cellular and Molecular Life Sciences*, vol. 65, no. 24, pp. 3961–3970, 2008.

[27] T. Kimura and T. Kambe, "The functions of metallothionein and ZIP and ZnT transporters: an overview and perspective," *International Journal of Molecular Sciences*, vol. 17, no. 3, Article ID 336, 2016.

[28] T. Kambe, K. M. Taylor, and D. Fu, "Zinc transporters and their functional integration in mammalian cells," *Journal of Biological Chemistry*, vol. 296, Article ID 100320, 2021.

[29] S. Yin, M. Duan, B. Fang, G. Zhao, X. Leng, and T. Zhang, "Zinc homeostasis and regulation: zinc transmembrane transport through transporters," *Critical Reviews in Food Science and Nutrition*, vol. 63, no. 25, pp. 7627–7637, 2023.

[30] N. H. McCormick and S. L. Kelleher, "ZnT4 provides zinc to zinc-dependent proteins in the *trans*—Golgi network critical for cell function and Zn export in mammary epithelial cells," *American Journal of Physiology-Cell Physiology*, vol. 303, no. 3, pp. C291–C297, 2012.

[31] S.-T. Lo, D. Parrott, M. V. C. Jordan et al., "The roles of ZnT1 and ZnT4 in glucose-stimulated zinc secretion in prostate epithelial cells," *Molecular Imaging and Biology*, vol. 23, no. 2, pp. 230–240, 2021.

[32] J. Adulcikas, S. Norouzi, L. Bretag, S. S. Sohal, and S. Myers, "The zinc transporter SLC39A7 (ZIP7) harbours a highly-conserved histidine-rich N-terminal region that potentially contributes to zinc homeostasis in the endoplasmic reticulum," *Computers in Biology and Medicine*, vol. 100, pp. 196–202, 2018.

[33] T. Nimmanon, S. Ziliotto, S. Morris, L. Flanagan, and K. M. Taylor, "Phosphorylation of zinc channel ZIP7 drives MAPK, PI3K and mTOR growth and proliferation signalling," *Metallomics*, vol. 9, no. 5, pp. 471–481, 2017.

[34] A. M. Downey, B. F. Hales, and B. Robaire, "Zinc transport differs in rat spermatogenic cell types and is affected by treatment with cyclophosphamide," *Biology of Reproduction*, vol. 95, no. 1, pp. 1–12, 2016.

[35] S. R. Powell, "The antioxidant properties of zinc," *The Journal of Nutrition*, vol. 130, no. 5, pp. 1447S–1454S, 2000.

[36] N. Liu, H. Xu, Q. Sun et al., "The role of oxidative stress in hyperuricemia and xanthine oxidoreductase (XOR) inhibitors," *Oxidative Medicine and Cellular Longevity*, vol. 2021, Article ID 1470380, 15 pages, 2021.

[37] D. Agnoletti, A. F. G. Cicero, and C. Borghi, "The impact of uric acid and hyperuricemia on cardiovascular and renal systems," *Cardiology Clinics*, vol. 39, no. 3, pp. 365–376, 2021.

[38] Y. Deng, F. Liu, X. Yang, and Y. Xia, "The key role of uric acid in oxidative stress, inflammation, fibrosis, apoptosis, and immunity in the pathogenesis of atrial fibrillation," *Frontiers in Cardiovascular Medicine*, vol. 8, Article ID 641136, 2021.

[39] M.-E. Gherghina, I. Peride, M. Tiglis, T. P. Neagu, A. Niculae, and I. A. Checherita, "Uric acid and oxidative stress—relationship with cardiovascular, metabolic, and renal impairment," *International Journal of Molecular Sciences*, vol. 23, no. 6, Article ID 3188, 2022.

[40] C.-Y. Deng, M. Lv, B.-H. Luo, S.-Z. Zhao, Z.-C. Mo, and Y.-J. Xie, "The role of the PI3K/AKT/mTOR signalling pathway in male reproduction," *Current Molecular Medicine*, vol. 21, no. 7, pp. 539–548, 2021.

[41] Y. Kimura, T. Yanagida, A. Onda, D. Tsukui, M. Hosoyamada, and H. Kono, "Soluble uric acid promotes atherosclerosis via AMPK (AMP-activated protein kinase)-mediated inflammation," *Arteriosclerosis, Thrombosis, and Vascular Biology*, vol. 40, no. 3, pp. 570–582, 2020.

[42] T. O. Crişan, M. C. P. Cleophas, B. Novakovic et al., "Uric acid priming in human monocytes is driven by the AKT–PRAS40 autophagy pathway," *Proceedings of the National Academy of Sciences*, vol. 114, no. 21, pp. 5485–5490, 2017.

[43] Y. Zhao, Y. Qian, Z. Sun et al., "Role of PI3K in the progression and regression of atherosclerosis," *Frontiers in Pharmacology*, vol. 12, Article ID 632378, 2021.

[44] Z. Xu, X. Han, D. Ou et al., "Targeting PI3K/AKT/mTOR-mediated autophagy for tumor therapy," *Applied Microbiology and Biotechnology*, vol. 104, no. 2, pp. 575–587, 2020.